



Universiteit
Leiden
The Netherlands

Safeguarding ovarian tissue autotransplantation in cancer patients

Peters, I.T.A.

Citation

Peters, I. T. A. (2018, January 10). *Safeguarding ovarian tissue autotransplantation in cancer patients*. Retrieved from <https://hdl.handle.net/1887/58923>

Version: Not Applicable (or Unknown)

License: [Licence agreement concerning inclusion of doctoral thesis in the Institutional Repository of the University of Leiden](#)

Downloaded from: <https://hdl.handle.net/1887/58923>

Note: To cite this publication please use the final published version (if applicable).

Cover Page



Universiteit Leiden



The handle <http://hdl.handle.net/1887/58923> holds various files of this Leiden University dissertation.

Author: Peters I.T.A.

Title: Safeguarding ovarian tissue autotransplantation in cancer patients

Issue Date: 2018-01-10



Chapter 5

Noninvasive detection of metastases and follicle density in ovarian tissue using full-field optical coherence tomography

Inge T.A. Peters*, Paulien L. Stegehuis*, Ronald Peek, Florine L. Boer, Erik W. van Zwet, Jeroen Eggermont, Johan R. Westphal, Peter J.K. Kuppen, J. Baptist Trimbos, Carina G.J.M. Hilders, Boudewijn P.F. Lelieveldt, Cornelis J.H. van de Velde, Tjalling Bosse, Jouke Dijkstra, Alexander L. Vahrmeijer

* These authors contributed equally to this article

Clin Cancer Research 2016;22(22):5506-5513

Abstract

Purpose

Autotransplantation of ovarian tissue can be used to restore fertility in cancer patients following gonadotoxic treatment. Whether this procedure is safe remains unclear, as current tumor detection methods render the ovarian tissue unsuitable for transplantation. Full-field optical coherence tomography (FF-OCT) is an imaging modality that rapidly produces high-resolution histology-like images without the need to fix, freeze, or stain the tissue. In this proof-of-concept study, we investigated whether FF-OCT can be used to detect metastases in ovarian tissue, thereby increasing the safety of ovarian tissue autotransplantation. We also evaluated whether cortical ovarian tissue and follicles remain viable following FF-OCT imaging.

Experimental design

Formalin-fixed, paraffin-embedded tissue samples were obtained from seven normal ovaries and fourteen ovaries containing metastases and/or micrometastases. These samples were deparaffinized and imaged using FF-OCT. The FF-OCT images were then compared to corresponding hematoxylin-and-eosin-stained tissue sections. Finally, we examined the effect of FF-OCT imaging on the viability of ovarian tissues and follicles in fresh bovine ovarian tissue using a glucose uptake and neutral red staining, respectively.

Results

FF-OCT illustrated both normal structures and metastases in ovarian tissue within minutes. Primordial follicles were readily identifiable. Finally, tissues and follicles remained viable following FF-OCT imaging for up to 180 and 60 minutes, respectively.

Conclusion

FF-OCT imaging is a promising method for the non-invasive detection of metastases, including micrometastases, in ovarian tissue. Moreover, this method facilitates the selection of cortical ovarian tissue with the highest density of primordial follicles, potentially increasing the likelihood of restoring ovarian function following ovarian tissue autotransplantation.

Introduction

Although advanced screening methods and novel treatment modalities represent a great leap forward in the treatment of cancer leading to substantially increased survival rates, new concerns have arisen as a consequence of these remedies, particularly among young women. Specifically, chemotherapy and/or pelvic radiotherapy can lead to premature ovarian failure due to accelerated follicle loss.¹ Therefore, preserving female reproductive capability is extremely important and has high priority. Currently, the most established fertility preservation procedures include freezing of embryos and/or oocytes. In addition, cryopreservation and subsequent autotransplantation of cortical ovarian tissue has become more prevalent. Because this method obviates the need for hormonal stimulation, it is deemed particularly suitable for prepubescent girls and young women who cannot delay the start of adjuvant therapy.² Autotransplantation of frozen-thawed ovarian tissue has been shown to restore ovarian activity in 93% of cases, and to date 60 resulting live births have been reported worldwide.³⁻⁴ Despite these encouraging statistics, the safety of this procedure cannot yet be ascertained for certain types of cancer, as there is a potential risk of occult ovarian involvement at the time of tissue harvesting.⁵⁻⁶ Due to the fact that the current tumor detection methods (e.g. histology, PCR analysis) render the tissue fragment unsuitable for transplantation, the presence of disseminated tumor cells can only be determined in the ovarian tissues that are ultimately not transplanted. Consequently, tumor cells that have metastasized to the actual ovarian autografts can be reimplanted, thereby potentially re-establishing cancer in the recipient. Previous reports have documented recurrences following autotransplantation in a patient diagnosed with breast cancer⁷ and a patient diagnosed with cervical cancer.⁸ However, whether these recurrences can be directly attributed to autotransplantation remains unclear. On the other hand, it is entirely plausible that malignant cells were reintroduced by autotransplantation in a patient with a granulosa cell tumor.⁹

To minimize the likelihood of reintroducing tumor cells, a technique that is capable of discriminating malignant from healthy tissues while leaving the examined tissues unaffected is needed. Full-field optical coherence tomography (FF-OCT) is a promising new imaging modality that satisfies these key criteria. Importantly, FF-OCT rapidly generates high-resolution histology-like images without the need to fix, freeze, or stain the tissue.¹⁰ With FF-OCT, the image contrast is based on the light-scattering properties of different structures in the tissue. FF-OCT has already been used successfully to detect tumors in a wide variety of human tissues, including prostate,¹¹ skin,¹² brain,¹³ lung,¹⁴ and kidney¹⁵ samples.

In this proof-of-concept study, we investigated whether FF-OCT can be used to visualize normal structures as well as metastases—including micrometastases—in human ovarian tissue. In addition, we evaluated whether cortical ovarian tissue and preantral follicles remain viable following FF-OCT imaging.

Materials and methods

Human ovarian tissue specimens

Formalin-fixed, paraffin-embedded (FFPE) specimens of normal ovaries obtained from premenopausal women who underwent prophylactic bilateral oophorectomy because of the presence of a *BRCA* gene mutation in the period 2001-2012 were selected from the archives of the Department of Pathology at the Leiden University Medical Center (LUMC). Patients who were previously treated with chemotherapy or used oral contraceptives prior to oophorectomy were excluded in order to ensure that only functionally active ovaries were included in the study. In addition, via a nationwide search performed by PALGA, the Dutch histopathology and cytopathology network and archive that covers all pathology laboratories within the Netherlands,¹⁶ FFPE specimens of ovarian metastases were collected from women with primary invasive breast cancer at age < 41 years in the period 2000-2010. Ovarian metastases derived from other primary malignancies in which ovarian tissue cryopreservation is performed were collected from the archives of the Department of Pathology at the LUMC. Hematoxylin-and-eosin (H&E) stained tissue sections were obtained and digitized using an IntelliSite Pathology Ultra-Fast scanner 1.6 RA (Philips, Eindhoven, the Netherlands). Following this, the entire FFPE tissue blocks were deparaffinized and imaged using FF-OCT.

All patient samples and clinical data were handled in accordance with the medical ethics guidelines described in the Code of Conduct for the Proper Secondary Use of Human Tissue of the Dutch Federation of Biomedical Scientific Societies (FMWV).¹⁷

Bovine ovarian tissue specimens

Intact bovine ovaries were collected at an abattoir within 15 minutes after slaughtering and immediately transported on ice to the laboratory at the LUMC. The average transport time was 20 minutes. At the laboratory, each ovary was cut into two halves, and the medulla was removed. The remaining cortex was trimmed to a thickness of 1-2 mm and subsequently cut into fragments measuring 2-3 mm or 5-10 mm in diameter for a glucose uptake assay or a neutral red staining, respectively. Bovine cortical ovarian fragments were stored until imaging (ranging from 0 to 180 minutes) in 24-wells plates at 4°C. Each well contained 1.5 ml DMEM culture medium (Lonza BioPharma; Visp, Switzerland) supplemented with 10% FCS (Gibco, Thermo-Fisher; Waltham, MA) and 1% penicillin/streptomycin (MP Biomedicals; Santa Ana, CA).

Full-field optical coherence tomography

A commercially available LightCT FF-OCT system (LLTech; Paris, France) was initially used in this study.¹⁸ During the course of the study, the LightCT scanner was upgraded to a newly developed FF-OCT system (LLTech), which is faster and can accommodate larger tissue samples. Both systems consisted of an upright microscope with a 10x objective with a central wavelength of 700 nm

with spectral width of 125 nm, and reference arm in the Linnik interferometric configuration.¹⁹⁻²⁰ The light reflected by the tissue interferes with the light reflected by the reference mirror, and the signal is then isolated from the scattered background light using a combination of four phase-shifted interferometric images. The LightCT scanner, which was used for the viability experiments, uses a 150-Watt white halogen lamp as the light source and generates a 0.8 mm x 0.8 mm *en face* image (with a maximum field of view 25 mm in diameter using image mosaicking) at an image rate of 35 Hz. The newly developed FF-OCT system, which was used to image the human ovarian tissues, uses an LED lamp as the light source and generates a 1.3 mm x 1.3 mm *en face* image (with a maximum field of view 45 mm in diameter) at an image rate of 75 Hz.

Image acquisition was similar for the two systems. In brief, the tissue was placed in the sample holder. Deparaffinized ovarian tissue was covered with saline, whereas fresh ovarian tissue was covered with DMEM culture medium (Lonza BioPharma) supplemented with 10% FCS (Gibco, Thermo-Fisher) and 1% penicillin/streptomycin (MP Biomedicals). An optical window was positioned above the tissue, and the tissue was gently flattened against this window. A layer of silicone oil was then applied between the optical window and the microscope objective. A macroscopic image was obtained using a wide-field camera, followed by FF-OCT images, which were made *en face*. The field of view encompassed the entire cortical ovarian fragment. With respect to human ovarian tissues, images were taken at a depth of 0-20 μm to ensure the best possible correspondence with the histology images. Considering the bovine cortical ovarian fragments, images were taken up to a depth of 100 μm , as it was the maximum depth at which high resolution could be retained. The number of images taken in depth depended on the time that was needed to achieve the predefined imaging time for the viability tests (ranging from 0 to 180 minutes). Both systems had 1.5 μm transverse resolution and 1 μm axial resolution.

Determining the viability of ovarian tissue using the glucose uptake assay

Bovine cortical ovarian tissue fragments measuring 2-3 mm in diameter were imaged using the LightCT scanner for 3, 10, 60, or 180 minutes. Fresh cortical ovarian samples that were not imaged served as a control, whereas cortical ovarian tissue samples in which cell death was induced by snap-freezing in liquid nitrogen served as a negative control. After imaging, the ovarian samples were transferred to 24-well plates for culturing. Each well was prepared in triplicate and contained three cortical ovarian samples in 1.5 ml DMEM culture medium (Lonza) supplemented with 10% FCS (Gibco, Thermo-Fisher) and 1% penicillin/streptomycin (MP Biomedicals). During culture, the medium was checked periodically for the presence of bacteria under a light microscope. The glucose content of the culture medium was measured using a blood-gas analyzer (Modular P Chemistry Analyzer; Roche Diagnostics, Indianapolis, IN). After four days in culture, the samples were weighed, and glucose consumption was measured and expressed per milligram of ovarian tissue per day, as previously described.²¹⁻²²

Determining the viability of ovarian follicles using neutral red staining

The viability of preantral ovarian follicles was determined using a neutral red staining assay adapted from the protocol published by Kristensen et al.²³ Fresh bovine cortical ovarian fragments were imaged in triplicate using the LightCT scanner for 3, 10, 60, or 180 minutes. These ovarian fragments were 5-10 mm in diameter and 1-2 mm thick. Fresh cortical ovarian fragments that were not imaged served as a control, and cortical ovarian tissue fragments in which cell death was induced by snap-freezing in liquid nitrogen served as a negative control. After imaging, the ovarian fragments were cut into small pieces. These pieces were placed in 15-ml conical tubes containing 5 ml preheated Serum-free Ultraculture medium (Lonza) supplemented with 1 mg/ml collagenase type IA (Sigma-Aldrich, St. Louis, MO). During incubation, the cell suspensions were triturated through a 5-ml pipette to further disrupt the tissue. After incubation for 25 minutes at 37°C, the samples were centrifuged at 2500 rpm for 5 minutes. The supernatants were poured off, and each pellet of cells was incubated for 1.5 hours at 37°C in 4.8 ml McCoy's medium (Life Technologies, Carlsbad, CA) supplemented with 2 µl Albuman (200 g/L; Sanquin, Amsterdam, the Netherlands), 50 µl Insulin-Transferrin-Selenium (ITS-G; Life Technologies), 50 µl penicillin/streptomycin (MP Biomedicals), and 75 µl neutral red solution (3.3 g/L; Sigma-Aldrich). The number of red-colored (viable) and uncolored (non-viable) follicles in the partially dissolved ovarian tissue fragments were counted in ten high-power fields per specimen under a light microscope by two independent observers (I.P. and P.S.) who were blinded with respect to the samples.

Statistical analysis

Statistical analysis was performed using SPSS version 23.0 (IBM, Armonk, NY). Inter-observer agreement was calculated using the Pearson correlation coefficient. A multivariate linear regression model was used to compute the mean difference in the glucose uptake of cortical ovarian biopsies between the various FF-OCT exposure times. The values were adjusted for the number of ovaries included. To investigate the effect of FF-OCT imaging on the viability of preantral follicles, we compared the proportions of viable preantral follicles between the various FF-OCT exposure times.

Results

Human ovarian tissue specimens

FFPE tissue samples from seven normal ovaries (obtained from six premenopausal patients) and fourteen ovaries containing metastases and/or micrometastases (obtained from twelve patients) were deparaffinized and imaged using FF-OCT. In most cases, the FF-OCT images could be easily interpreted using the inverse setting. In this inverse setting, structures that reflect light the strongest appear black, whereas structures that reflect light poorly appear white.

Figure 1 shows representative FF-OCT images and corresponding histology images of the most clinically relevant structures in a normal ovary. The primordial follicles, which are small primary oocytes surrounded by a single layer of flattened granulosa cells,²⁴ appear as either round or crescent-shaped white structures, depending on the level at which they were imaged (Figure 1A-B). In primary follicles, the flat granulosa cells transform into a cuboidal structure and the zona pellucida forms between this layer and the oocyte. On the FF-OCT image, the oocyte appears somewhat darker than the zona pellucida, and the granulosa cells can be distinguished quite well (Figure 1C-D). Figure 1E-F shows a corpus rubrum, which is a small hemorrhage that forms immediately after ovulation. The corpus luteum is composed of an outer layer of smaller thecal-lutein cells and an inner layer of larger granulosa-lutein cells. On the FF-OCT images, the densely packed thecal-lutein cells reflected more light than the granulosa-lutein cells, which reflected light to the same extent as the corpus rubrum (Figure 1G-H). The corpus albicans (Figure 1I-J) and corpus fibrosum (Figure 1K-L), which are masses of fibrous scar tissues that form when the oocyte is not fertilized, showed high levels of reflection due to their collagen content. Lastly, an inclusion cyst (Figure 1M-N) was identified by its thin dark outer layer and lack of interior structure.

Figure 2A shows representative FF-OCT images of a sagittal section of an ovary containing micrometastases; this sample was derived from a primary invasive ductal breast carcinoma. Figure 2B-C and Figure 2D-E show magnified views of micrometastases measuring 0.9 mm and 1.7 mm, respectively. These metastatic lesions could be distinguished clearly from the surrounding stromal cells, as the stromal cells reflected considerably more light than the lesions. On the FF-OCT images, these lesions have a 'web-like' architecture in which the tumor cells appear light gray. Furthermore, a distorted ovarian cortex architecture (Figure 2D) was often seen in the presence of disseminated tumor cells. Figure 3 shows metastatic lesions within ovarian tissues obtained from three individual patients. Figure 3A-B depicts a solitary metastasis that originated from an invasive ductal breast carcinoma; the FF-OCT image shows the microglandular proliferation. In Figure 3C-D, the ovarian stroma is completely occupied by the metastatic lesion, which has a characteristic stromal component. The FF-OCT image of a metastasis originating from a primary endometrial carcinoma shows a typical cribriform morphology (Figure 3E), with good correspondence with the previously obtained H&E tissue section (Figure 3F). The morphological features of the remaining ten ovaries containing metastatic disease corresponded to those depicted in Figures 2 and 3. All types of normal ovarian features and metastatic lesions that were identified in the histology (H&E) sections were also detected by FF-OCT.

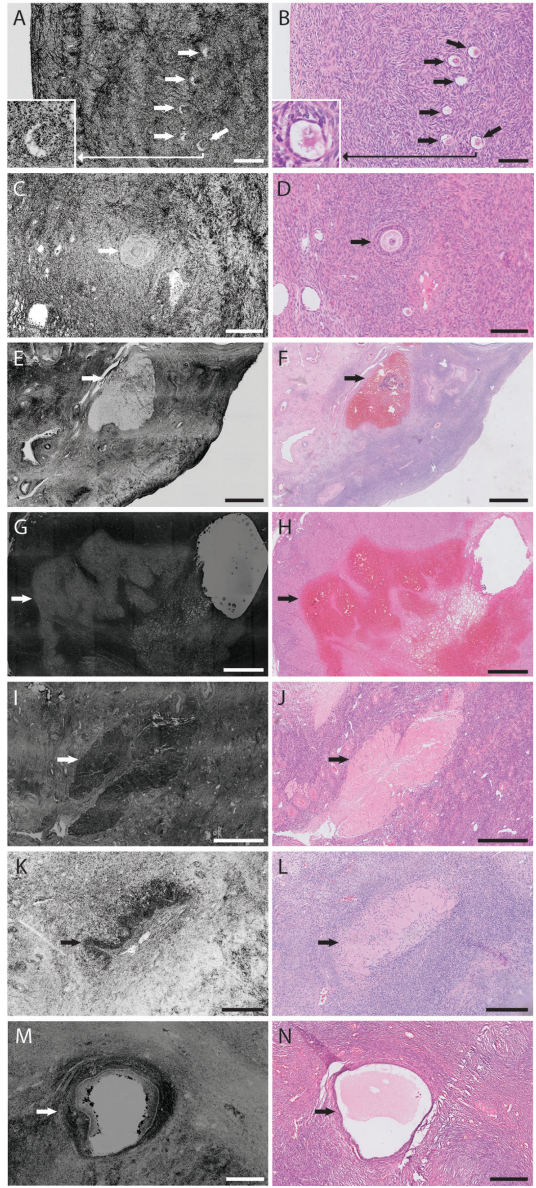


Figure 1. Example inverse FF-OCT images (left column) and corresponding histology images (right column) of normal ovarian tissues

The following normal ovarian structures are shown in the images: primordial follicles (A-B), a primary follicle (C-D), a corpus rubrum (E-F), part of a corpus luteum (G-H), a corpus albicans (I-J), a corpus fibrosum (K-L), and an inclusion cyst (M-N). In each image, the normal ovarian structures are indicated by an arrow. All but one primordial follicle were detected in the FF-OCT image (A) as compared to the corresponding histology image (B). This is due to a slightly different imaging depth. Scale bars represent 100 μm (A-B), 150 μm (C-D), 250 μm (K-L, and M-N), and 1 mm (E-F, G-H, and I-J). Insets show a characteristic primordial follicle (A-B) at three times higher magnification.

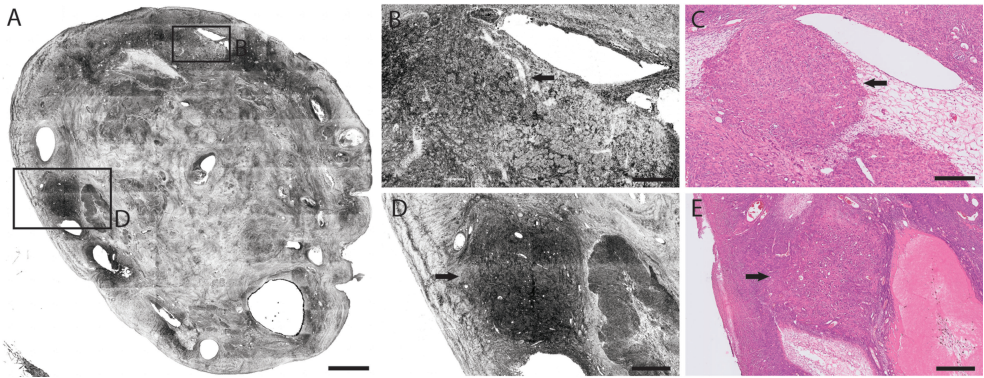


Figure 2. Example inverse FF-OCT images and corresponding histology images of ovarian metastases originating from a primary invasive ductal breast carcinoma

A sagittal view is shown in panel A, and panels B-E show magnified views of the micrometastases (indicated by arrows). Scale bars represent 2 mm (A), 250 μm (B-C), and 500 μm (D-E).

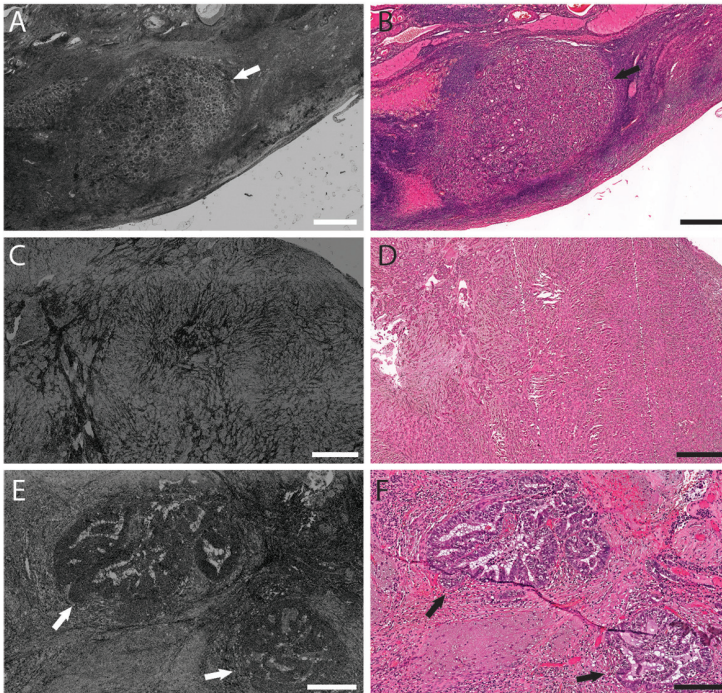


Figure 3. Example inverse FF-OCT images (left column) and corresponding histology images (right column) of ovarian metastases

An ovary containing a solitary metastasis originating from a primary invasive breast carcinoma is shown in panels A and B (indicated by arrows). An ovary in which disseminated breast tumor cells are dispersed throughout the ovary is shown in panels C and D. Micrometastases originating from a primary endometrial carcinoma are shown in panels E and F (indicated by arrows). Scale bars represent 500 μm (A-D) and 200 μm (E-F).

Viability of ovarian tissue measured using a glucose uptake assay

Next, we examined whether performing FF-OCT imaging on fresh cortical ovarian tissue affects tissue viability. Table 1 shows the mean glucose consumption per mg ovarian tissue per day over a 4-day culture period of the fresh cortical ovarian tissues that were imaged using FF-OCT for 0, 3, 10, 60, and 180 minutes. All values were adjusted for the number of ovaries used, and none reached statistical significance. Thus, cortical ovarian tissue remained viable — at least with respect to glucose uptake — up to three hours of FF-OCT imaging. No glucose uptake was measured in the cortical ovarian biopsies in which cell death was induced.

Table 1. Viability of cortical ovarian tissue after different FF-OCT exposure times

	Glucose uptake (mmol/mg tissue/day)	
	Mean	95% CI ^a
FF-OCT imaging time		
0 minutes	50.52	42.66 - 58.38
3 minutes	46.49	38.63 - 54.35
10 minutes	44.25	36.40 - 52.11
60 minutes	40.32	32.46 - 48.18
180 minutes	46.25	38.39 - 54.11

^a CI; confidence interval

The mean glucose uptake over a 4-day culture period was determined in triplicate, as described in the material and methods section. All values were adjusted for the various ovaries, using a multivariate linear regression model, resulting in a standard error of the mean of 4.01.

Viability of preantral ovarian follicles measured using neutral red staining

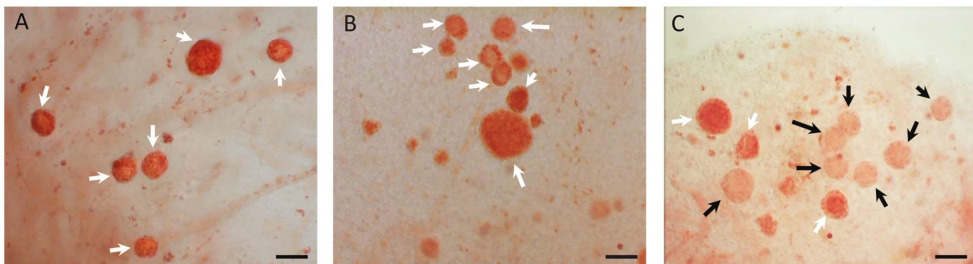
We also examined the effect of different FF-OCT exposure times on the viability of preantral follicles in fresh cortical ovarian tissue fragments using neutral red staining. The percentage of viable preantral follicles in the samples that were not subjected to FF-OCT imaging was 86% (95% CI 0.81-0.92; Table 2). Although some variation was observed, this viability did not significantly decrease following FF-OCT imaging for up to 60 minutes. Cortical ovarian tissue fragments that were exposed to FF-OCT for 180 minutes had a significantly lower percentage (55%) of viable preantral follicles. As a negative control, no viable preantral follicles were observed in the cortical ovarian tissues in which cell death was induced. Figure 4 shows representative examples of preantral follicles in fresh cortical ovarian tissues that were not exposed to FF-OCT imaging (Figure 4A), preantral follicles that were subjected to FF-OCT imaging for 10 minutes (maximum time required to image a cortical ovarian fragment; Figure 4B) and preantral follicles that were exposed to FF-OCT imaging for 180 minutes (Figure 4C).

Table 2. Viability of preantral follicles after different FF-OCT exposure times

	Total number of follicles observed	Total number of viable follicles	Proportion	95% CI ^a
FF-OCT imaging time				
0 minutes	145	125	0.86	0.81 - 0.92
3 minutes	208	183	0.88	0.84 - 0.92
10 minutes	193	189	0.98	0.96 - 1.00
60 minutes	195	185	0.95	0.92 - 0.98
180 minutes	179	99	0.55	0.48 - 0.63

^a CI; confidence interval

The proportion of viable preantral follicles was determined by a neutral red staining. Results are based on three different cortical ovarian fragments per condition.

**Figure 4. Viability of preantral follicles before and after FF-OCT imaging**

Representative images of preantral follicles in fresh cortical ovarian tissues that were not exposed to FF-OCT imaging are shown in panel A. Preantral follicles in cortical ovarian tissues that were subjected to FF-OCT imaging for 10 minutes are shown in panel B. Preantral follicles in cortical ovarian tissues that were subjected to FF-OCT imaging for 180 minutes are shown in panel C. The white and black arrows indicate red-colored (i.e., viable) and uncolored (i.e., non-viable) follicles, respectively. Scale bars represent 100 μ m.

Discussion

In this proof-of-concept study, we investigated whether FF-OCT can be used to detect metastases in ovarian tissue prior to autotransplantation, thereby reducing the risk of reintroducing ovarian tissue that might contain metastases. We found that FF-OCT can be used to visualize both normal structures and metastases — including micrometastases — in ovarian tissues derived from premenopausal women. These findings are particularly relevant from a clinical perspective, given that the pathologist must distinguish between benign and malignant lesions based solely on tomographic images. Routine pathology methods such as histology and immunohistochemistry cannot be used in this context, as these methods render the cortical ovarian tissue unsuitable for autotransplantation. Importantly, our results may serve to help pathologists use FF-OCT as a novel tool for detecting metastases in ovarian tissues.

In our study, we used deparaffinized FFPE tissue samples, as fresh ovarian tissues were not readily available for research purposes and ovarian metastases are relatively rarely encountered. However, we found no difference with respect to visual assessment of normal ovarian structures between the deparaffinized ovarian tissue samples and the fresh ovarian tissues that were used for measuring viability. Our finding is supported by a study of Wilson et al. in which the optical features of various non-paraffinized and deparaffinized tissues were compared and no substantial differences were found.²⁵

Because of the relatively few number of ovarian tissue samples that contained micrometastases, we were unable to perform a blinded analysis in which two pathologists independently assessed the FF-OCT images without having access to the original H&E-stained tissue sections. Such an analysis would require a 'training set' in order to familiarize the pathologists with non-neoplastic and neoplastic ovarian tissues on FF-OCT, followed by a 'test set' for which the sensitivity and specificity of FF-OCT imaging could be determined.¹⁴⁻¹⁵ Although this type of analysis was beyond the scope of this proof-of-concept study, it should be performed in future studies in order to confirm whether FF-OCT is a suitable diagnostic instrument for use in ovarian tissue. The maximum depth of FF-OCT imaging that provided high-resolution images in the cortical ovarian strips was approximately 100 μm , which is considerably lower than the imaging depth of up to 500 μm reported for other tissues.¹⁰ This difference is due primarily to the large-scale extracellular matrix network in the ovarian cortex,²⁶⁻²⁷ which greatly reduces tissue penetration.²⁸ Nevertheless, imaging depth could be increased somewhat by imaging the cortical ovarian tissue fragments from both sides, thereby effectively doubling the amount of tissue that can be imaged. Moreover, rapid advances in the field of optical imaging will likely enable clinicians to use this non-invasive approach to visualize even deeper structures in the near future.

Interestingly, previous studies that used conventional OCT to examine ovaries achieved an imaging depth of up to 2 mm.²⁹⁻³⁰ However, the imaging resolution of conventional OCT is considerably lower than FF-OCT.³¹ For our purposes, achieving ultra-high resolution is crucial, as patients with clinically diagnosed early-stage cancer who are eligible for cryopreservation of ovarian tissue can potentially have occult micrometastases in their ovarian tissues.³²⁻³⁴ Importantly, FF-OCT imaging provides images with a resolution of approximately 1 μm .³¹ In addition to the detection of occult ovarian involvement, this high-resolution imaging modality provides the opportunity to visually assess the density of primordial follicles in the ovarian autografts, which is highly relevant, given that successfully restoring ovarian activity depends critically on the number of primordial follicles present in the ovarian autograft.³ Thus, FF-OCT provides the added value of selecting the cortical ovarian fragments with the highest potential for restoring fertility.

Because FF-OCT generates images at a rapid rate,¹⁵ this technique is particularly suitable to the field of ovarian tissue cryopreservation, where ischemia and oxidative stress during a lengthy avascular period are known to cause loss of primordial follicles.³⁵ The average time required to image a cortical ovarian fragment measuring 5-10 mm in diameter was seven minutes using the

original FF-OCT system, and this time was reduced further to a mere one minute with the newly developed FF-OCT system. During these brief periods, the viability of both the ovarian tissue and the preantral follicles remained high. Even performing FF-OCT imaging for 180 and 60 minutes did not significantly reduce the viability of ovarian tissues and preantral follicles, respectively. These data support the notion that short-term FF-OCT imaging has little effect on either ovarian tissues or preantral follicles. Nevertheless, given that the most meaningful outcome in the field of fertility preservation is ultimately a successful pregnancy, future research will focus on evaluating pregnancy rates following exposure to FF-OCT.

With respect to using FF-OCT as a non-invasive means to detect metastases in the actual ovarian autografts, cortical ovarian strips can be imaged immediately following oophorectomy (see the proposed workflow diagram in Supplementary Figure 1). If the pathologist observes lesions that raise a suspicion of metastases, these fragments could then be analyzed further using histological examination and/or PCR analysis. If these further tests confirm the presence of metastatic tissue in the ovarian fragments, no autotransplantation will be performed. On the other hand, if the histological results are negative (i.e., a false positive result on FF-OCT), the remaining ovarian fragments—particularly those fragments that appeared normal on FF-OCT imaging—can still be transplanted. Moreover, as discussed above, the pathologist can also select the tissue fragments with the highest density of follicles, thereby maximizing the likelihood of restoring the patient's ovarian function. Importantly, FF-OCT imaging should be performed under sterile conditions in order to prevent bacterial contamination.

In conclusion, FF-OCT imaging is a promising new non-invasive method for rapidly detecting ovarian metastases in ovarian fragments prior to autotransplantation in patients whose ovarian function has been lost. Moreover, this method facilitates the selection of cortical ovarian tissues with the highest density of primordial follicles, significantly increasing the likelihood of restoring ovarian function. Although it is not yet possible to detect all ovarian metastases and/or follicles in the cortical ovarian fragments due to a limited tissue penetration depth, FF-OCT provides a large improvement over the current tumor detection methods as it is the only approach now available by which the actual ovarian autografts, used for transplantation, can be examined.

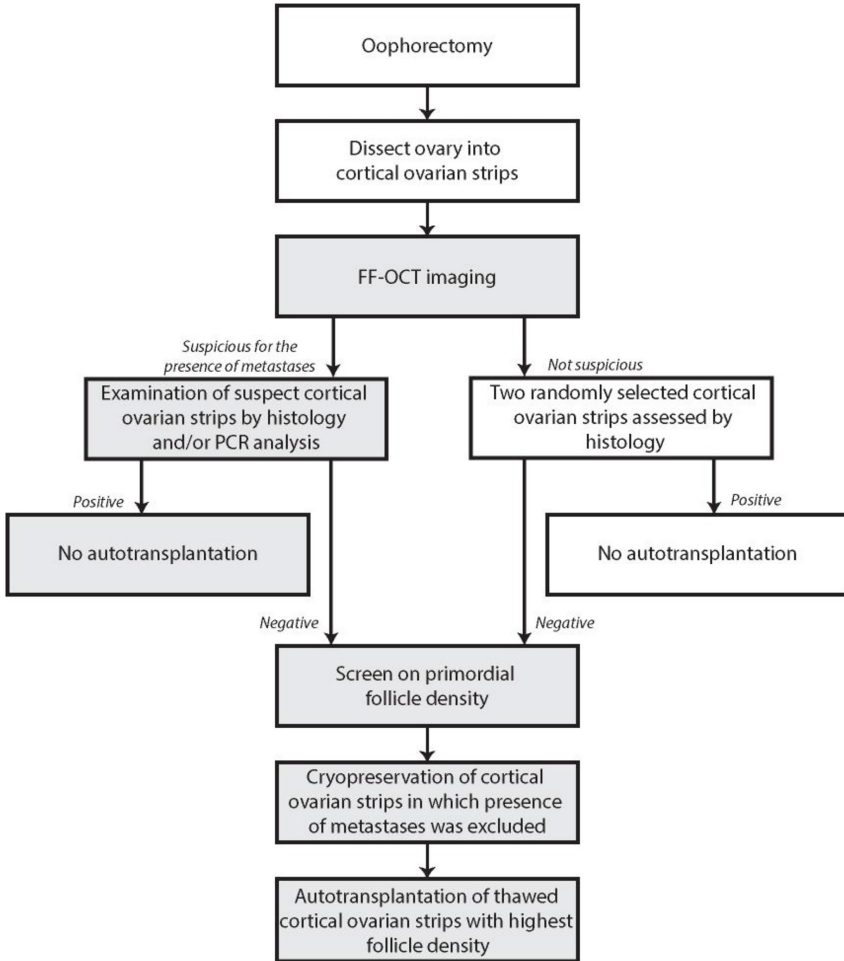
Acknowledgements

The authors are grateful to the Dutch Pathology Registry (PALGA) and the pathology laboratories for their collaboration. The authors also thank the Clinical Chemistry Laboratory at the Leiden University Medical Center for providing practical help.

References

- Morgan S, Anderson RA, Gourley C, Wallace WH, Spears N. How do chemotherapeutic agents damage the ovary? *Hum Reprod Update* 2012;18(5):525-535.
- The Practice Committee of the American Society for Reproductive Medicine. Ovarian tissue cryopreservation: a committee opinion. *Fertil Steril* 2014;101(5):1237-1243.
- Donnez J, Dolmans MM, Pellicer A, et al. Restoration of ovarian activity and pregnancy after transplantation of cryopreserved ovarian tissue: a review of 60 cases of reimplantation. *Fertil Steril* 2013;99(6):1503-1513.
- Donnez J, Dolmans MM. Ovarian cortex transplantation: 60 reported live births brings the success and worldwide expansion of the technique towards routine clinical practice. *J Assist Reprod Genet* 2015;32(8):1167-1170.
- Dolmans MM, Luyckx V, Donnez J, Andersen CY, Greve T. Risk of transferring malignant cells with transplanted frozen-thawed ovarian tissue. *Fertil Steril* 2013;99(6):1514-1522.
- Bastings L, Beerendonk CCM, Westphal JR, et al. Autotransplantation of cryopreserved ovarian tissue in cancer survivors and the risk of reintroducing malignancy: a systematic review. *Hum Reprod Update* 2013;19(5):483-506.
- Ernst EH, Offersen BV, Andersen CY, Ernst E. Legal termination of a pregnancy resulting from transplanted cryopreserved ovarian tissue due to cancer recurrence. *J Assist Reprod Genet* 2013;30(7):975-978.
- Kim SS. Assessment of long term endocrine function after transplantation of frozen-thawed human ovarian tissue to the heterotopic site: 10 year longitudinal follow-up study. *J Assist Reprod Genet* 2012;29(6):489-493.
- Stern CJ, Gook D, Hale LG, et al. Delivery of twins following heterotopic grafting of frozen-thawed ovarian tissue. *Hum Reprod* 2014;29(8):1828.
- Harms F, Dalimier E, Vermeulen P, Fragola A, Boccarda AC. Multimodal full-field optical coherence tomography on biological tissue: toward all optical digital pathology. *Proc of Spie* 2012;8216:821609-1-8.
- Lopater J, Colin P, Beuvon F, et al. Real-time cancer diagnosis during prostate biopsy: ex vivo evaluation of full-field optical coherence tomography (FFOCT) imaging on biopsy cores. *World J Urol* 2016;34(2):237-243.
- Durkin JR, Fine JL, Sam H, Pugliano-Mauro M, Ho J. Imaging of Mohs micrographic surgery sections using full-field optical coherence tomography: a pilot study. *Dermatol Surg* 2014;40(3):266-274.
- Assayag O, Antoine M, Sigal-Zafrani B, et al. Large field, high resolution full-field optical coherence tomography: a pre-clinical study of human breast tissue and cancer assessment. *Technol Cancer Res Treat* 2014;13(5):455-468.
- Jain M, Narula N, Salamoon B, et al. Full-field optical coherence tomography for the analysis of fresh unstained human lobectomy specimens. *J Pathol Inform* 2013;4:26.
- Jain M, Robinson BD, Salamoon B, Thouvenin O, Boccarda C, Mukherjee S. Rapid evaluation of fresh kidney tissue with full-field optical coherence tomography. *J Pathol Inform* 2015;6:53.
- Casparie M, Tiebosch AT, Burger G, et al. Pathology databanking and biobanking in The Netherlands, a central role for PALGA, the nationwide histopathology and cytopathology data network and archive. *Cell Oncol* 2007;29(1):19-24.
- Federa FMWV. Code for proper secondary use of human tissue in the Netherlands 2002. Available from: <http://www.federa.org/codes-conduct>.
- LLTechimaging. LightCT FF-OCT system 2016. Available from: <http://www.lltechimaging.com/products-applications/products/>.
- Dubois A, Vabre L, Boccarda AC, Beaufrepaire E. High-resolution full-field optical coherence tomography with a Linnik microscope. *Appl Opt* 2002;41(4):805-812.
- Dubois A. Full-field optical coherence microscopy. In: Liu G, editor. Selected topics in optical coherence tomography. Rijeka, Croatia: InTech; 2012; 3-20.
- Gerritse R, Beerendonk CCM, Westphal JR, Bastings L, Braat DDM, Peek R. Glucose/lactate metabolism of cryopreserved intact bovine ovaries as a novel quantitative marker to assess tissue cryodamage. *Reprod Biomed Online* 2011;23(6):755-764.
- Bastings L, Liebenthron J, Westphal JR, et al. Efficacy of ovarian tissue cryopreservation in a

- major European center. *J Assist Reprod Genet* 2014;31(8):1003-1012.
23. Kristensen SG, Rasmussen A, Byskov AG, Andersen CY. Isolation of pre-antral follicles from human ovarian medulla tissue. *Hum Reprod* 2011;26(1):157-166.
 24. Gougeon A, Chainy GB. Morphometric studies of small follicles in ovaries of women at different ages. *J Reprod Fertil* 1987;81(2):433-442.
 25. Wilson JW, Degan S, Warren WS, Fischer MC. Optical clearing of archive-compatible paraffin embedded tissue for multiphoton microscopy. *Biomed Opt Express* 2012;3(11):2752-2760.
 26. Lind AK, Weijdegård B, Dahm-Kähler P, Mölne J, Sundfeldt K, Brännström M. Collagens in the human ovary and their changes in the perifollicular stroma during ovulation. *Acta Obstet Gynecol Scand* 2006;85(12):1476-1484.
 27. Laronda MM, Jakus AE, Whelan KA, Wertheim JA, Shah RN, Woodruff TK. Initiation of puberty in mice following decellularized ovary transplant. *Biomaterials* 2015;50:20-29.
 28. Trottmann M, Kölle S, Leeb R, et al. Ex vivo investigations on the potential of optical coherence tomography (OCT) as a diagnostic tool for reproductive medicine in a bovine model. *J Biophotonics* 2016;9(1-2):129-137.
 29. Brewer MA, Utzinger U, Barton JK, et al. Imaging of the ovary. *Technol Cancer Res Treat* 2004;3(6):617-627.
 30. Hariri LP, Bonnema GT, Schmidt K, et al. Laparoscopic optical coherence tomography imaging of human ovarian cancer. *Gynecol Oncol* 2009;114(2):188-194.
 31. Dubois A, Moreau J, Boccard C. Spectroscopic ultrahigh-resolution full-field optical coherence microscopy. *Opt Express* 2008;16(21):17082-17091.
 32. Azem F, Hasson J, Ben-Yosef D, et al. Histologic evaluation of fresh human ovarian tissue before cryopreservation. *Int J Gynecol Pathol* 2010;29(1):19-23.
 33. Sánchez-Serrano M, Novella-Maestre E, Roselló-Sastre E, Camarasa N, Teruel J, Pellicer A. Malignant cells are not found in ovarian cortex from breast cancer patients undergoing ovarian cortex cryopreservation. *Hum Reprod* 2009;24(9):2238-2243.
 34. Hoekman EJ, Smit VT, Fleming TP, Louwe LA, Fleuren GJ, Hilders CG. Searching for metastases in ovarian tissue before autotransplantation: a tailor-made approach. *Fertil Steril* 2014;103(2):469-477.
 35. Van Eyck AS, Jordan BF, Gallez B, Heilier JF, Van Langendonck A, Donnez J. Electron paramagnetic resonance as a tool to evaluate human ovarian tissue reoxygenation after xenografting. *Fertil Steril* 2009;92(1):374-381.



Supplementary Figure S1. Proposed clinical workflow for screening cortical ovarian strips prior to autotransplantation in order to minimize the likelihood of reintroducing tumor cells and maximize the likelihood of restoring ovarian function

The light-gray shaded boxes indicate steps in which FF-OCT imaging can provide added value.

